J. Fluid Mech. (1969), *vol.* 38, *part* 2, *pp.* 279–303
Printed in Great Britain

Finite bandwidth, finite amplitude convection

By ALAN C. NEWELL

Department of Planetary and Space Science,
Department of Mathematics

AND J. A. WHITEHEAD

Institute of Geophysics and Planetary Physics,
University of California, Los Angeles

(Received 19 July 1968 and in revised form 4 March 1969)

The main purpose of this work is to show how a continuous finite bandwidth of modes can be readily incorporated into the description of post-critical Rayleigh–Bénard convection by the use of slowly varying (in space and time) amplitudes. Previous attempts have used a multimodal discrete analysis. We show that in addition to obtaining results consistent with the discrete mode approach, there is a larger class of stable and realizable solutions. The main feature of these solutions is that the amplitude and wave-number of the motion is that of the most unstable mode almost everywhere, but, depending on external and initial conditions, the roll couplets in different parts of space may be 180° out of phase. The resulting discontinuities are smoothed by hyperbolic tangent functions. In addition, it is clear that the mechanism for propagating spatial nonuniformities is diffusive in character.

1. Introduction and general discussion

It is clear from the stability diagram (figure 1) of Rayleigh number *vs.* wave-number in the case of a motionless fluid heated from below that, for a given Rayleigh number greater than the critical Rayleigh number, a continuous finite band of modes in the neighbourhood of the critical wave-number (R_{cr}) may be excited. For example, if $(R-R_{cr})/R_{cr}$ (R the Rayleigh number) is $\epsilon^2\chi$, then a $O(\epsilon)$ band of modes is possible. Previous work such as that of Schlüter, Lortz & Busse (1965) and Segel (1966) are typical of attempts to examine possible finite amplitude solutions in that the analysis is carried through using a discrete modal synthesis in order to represent the flow fields. While extremely regular rolls have been observed in some supercritical experimental situations (Koschmieder 1966), in general the observed rolls have exhibited rather irregular patterns (Chen & Whitehead 1968; Silveston 1958). It is difficult to conceive that discrete multimodal solutions can allow a wide enough class of functions to describe the spatial amplitude modulations which inevitably occur as the result of non-uniform forcing or from general initial and boundary conditions. We attempt here to include a wider class of solutions by allowing the continuous band to be represented. The technique used is similar to that developed by Benney & Newell

(1967) for interacting wave packets and analogous to the averaging technique of Whitham (1965). The basic idea is to treat the amplitude W of the vertical velocity's neutral solution around $R = R_{\rm cr}$, $\mathbf{k} = \mathbf{k}_{\rm cr}$ as a slowly varying function of both position and time.

Insertion of this representation of the neutral solution into the non-linear equations leads to certain conditions having to be satisfied in order to successively solve the iteration equations. This solvability condition then yields an equation for $W(X, Y, T)$ ($X = \epsilon x$, $Y = \epsilon y$, $T = \epsilon^2 t$). In non-dimensional form, this reads

$$2\frac{p+1}{p}\frac{\partial W}{\partial T} - 8\,(\hat{\mathbf{n}}.\nabla_{\mathbf{x}})^2\,W = (3\pi^2\chi - WW^*)\,W, \tag{1.1}$$

where $\hat{\mathbf{n}}$ is the unit vector in the direction of a critical mode, and $p = \nu/\kappa$ is the Prandtl number.

The only difference in this equation from other approaches (for example, Segel 1966) is the presence of the diffusion term on the left-hand side. In the absence of this term the amplitudes would be driven to the stable stationary solution by the Van der Pol oscillator term on the right-hand side:

$$WW^* = 3\pi^2\chi. \tag{1.2}$$

Our first observation is that non-uniformities in space are propagated (in dimensional form) by diffusion according to the law

$$x \sim 4\sqrt{\left(\frac{p}{p+1}\kappa t\right)}, \tag{1.3}$$

where κ is the thermometric conductivity. In the limit of large Prandtl number (or small heat conductivity) the relevant diffusion time is that of heat conduction as the information that one roll is spinning is relayed to its neighbour by a thermal torque. On the other hand, for low Prandtl numbers (or high heat conductivity) the very fast propagation of temperature information suppresses the effect of the thermal torque in the neighbouring roll and the information is transmitted by viscous torques. We see from (1.3) that in the limit $p \to 0$

$$x \sim 4\sqrt{(\nu t)}.$$

Such diffusive behaviour has been observed in an apparatus described by Chen & Whitehead (1968). Shortly after the critical Rayleigh number was exceeded, one spot would begin to convect. If the critical Rayleigh number was only slightly exceeded so that small random disturbances elsewhere in the tank had not sufficient time to grow by themselves, the disturbance that first convected would diffuse outward, triggering neighbouring cells. In the very slow and careful experiment by Koschmieder (1966), the sidewall effect dominated the pattern of flow. We emphasize that once diffusion has triggered the disturbance, its subsequent growth depends additionally on the Van der Pol forcing. However, in many situations there is initially no significant spatial non-uniformity; in fact, the initial disturbances can be spatially random. In these situations the statistical initial value problem would be appropriate.

In §2, equations somewhat more general than (1.1) and appropriate for the

study of finite bandwidth convection are developed. The essential difference is that we treat modal packages instead of discrete modes. By a modal package we mean a local continuous band of wave-numbers centred on a discrete mode. The advantages of the approach are fully discussed. In § 3, we look at the modal solutions for the case of rolls and their stability. Although the approach is new, this part of the analysis closely resembles the work of Schlüter *et al.* (1965) and that of Eckhaus (1965). However, in addition, although we are in full agreement with the results of these authors on the stability bounds of modal solutions, we show that it is unlikely that modes other than the critical mode can ever reach their finite amplitude solutions if perturbed before they reach their finite amplitude state. Correlation of these analytic results with the experiment of Chen & Whitehead (1968) is discussed.

In § 4, we develop a completely new class of solutions and demonstrate in some limited cases their stability. Although reasonably complicated solutions can occur depending upon initial and boundary conditions, one of the essential features is that the rolls often reach the finite amplitude solutions of the critical modes lying on the circle $k^2 = \frac{1}{2}\pi^2$ of the neutral stability surface (see figure 2). This phenomenon manifests itself as solutions in which the modulus of the amplitude is that of the finite amplitude state of the neutral roll but where the sense of rotation of corresponding roll couplets differs in different parts of space. The discontinuities (which may be forced by external heating, initial or boundary conditions) are smoothed by boundary-layer-like hyperbolic tangent functions. In addition, in order for these solutions to be stable 'jetlike' profiles appear as the envelope solutions to the neutral modes which are 90° out of phase.

Finally we emphasize that although a discrete package representation is necessary in order to describe a full three-dimensional flow, in the two-dimensional case a single diffusion-like equation suffices to describe any flow. Several numerical solutions to this equation with various initial and boundary conditions were computed. The solutions obtained contained the essential feature described in the previous paragraph, namely that the shape of the steady solutions proved to be rectangular with discontinuities smoothed by hyperbolic tangent functions. However, the relevant scales of the final solution were closely related to the dominant scales of the initial conditions which were compatible with boundary conditions.

2. Equations of motion

The equations describing the perturbation fields about a stationary state for the problem of a fluid heated from below are relatively well known. Using the Boussinesq approximation and neglecting the heat produced by viscous dissipation, they are

$$\nabla . \mathbf{u} = 0, \tag{2.1}$$

$$\frac{\partial \mathbf{u}}{\partial t} + (\boldsymbol{\Omega} \times \mathbf{u}) = -\nabla\left(\frac{p}{\rho_r} + \tfrac{1}{2}\mathbf{u}.\mathbf{u}\right) + \alpha g \hat{\mathbf{z}} T + \nu \nabla^2 \mathbf{u}, \quad \boldsymbol{\Omega} = \nabla \times \mathbf{u}, \tag{2.2}$$

$$\frac{\partial T}{\partial t} + \mathbf{u}.\nabla T - \beta\omega = \kappa \nabla^2 T, \tag{2.3}$$

where $T(\mathbf{r},t)$, $p(\mathbf{r},t)$ and $u(\mathbf{r},t)$ are the perturbation temperature, pressure and velocity fields respectively; κ is the thermometric conductivity, ν the viscosity, $\hat{\mathbf{z}}$ the unit vector in the vertical direction, and $w = \mathbf{u}.\hat{\mathbf{z}}$. The motionless state is described by a linear temperature profile:

$$\frac{d\bar{T}(z)}{dz} = -\beta, \tag{2.4}$$

$$\frac{d\bar{p}(z)}{dz} = -\rho_r g\{1-\alpha(\bar{T}-T_r)\}, \tag{2.5}$$

$$\mathbf{u} = 0,$$

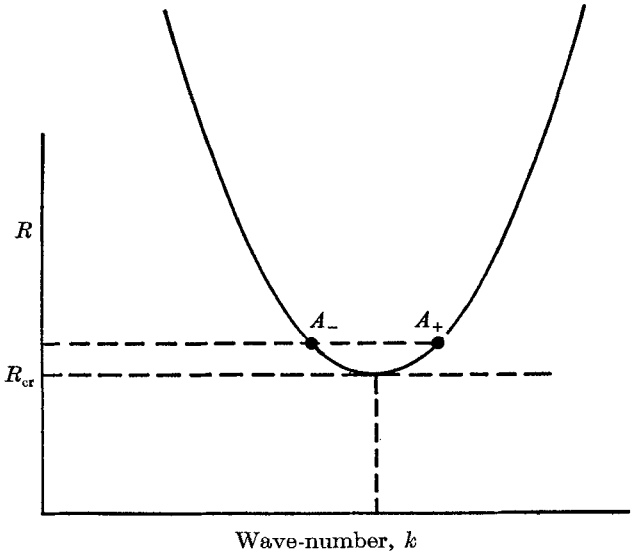

FIGURE 1. Stability diagram showing finite bandwidth of modes.

where α is the coefficient of cubic expansion of the fluid, and ρ_r, T_r are reference density and temperature. The co-ordinate z represents the vertical co-ordinate whereas x and y are the horizontal co-ordinates.

The usual stability problem associated with the above set of equations and appropriate boundary conditions is to find the lowest temperature gradient β_0 which allows non-damped solutions of the linearized equations. In the free–free boundary case with perfectly conducting boundaries, the boundary conditions are that

$$w = 0, \quad \frac{\partial^2 w}{\partial z^2} = 0, \quad T = 0, \quad \text{at} \quad z = 0, d. \tag{2.6}$$

It is readily shown that a disturbance of the form

$$e^{i\mathbf{k}.\mathbf{x}} \sin\frac{m\pi z}{d}$$

first becomes unstable for a Rayleigh number $\alpha g\beta_0 d^4/\kappa\nu$ (the non-dimensionalized temperature gradient) of $27\pi^4/4$ with the corresponding wave-numbers

$$k^2 = \pi^2/(2d^2), \quad m = 1.$$

The stability graph is shown in figure 1.

It is also known (Segel 1966) that for Rayleigh numbers R in the neighbourhood of the critical Rayleigh number R_{cr} (for the case of free–free boundaries with constant temperature gradient $R > R_{cr}$) that finite amplitude solutions can exist. There seems to have been little attention paid to the fact that for $R - R_{cr} = O(\epsilon^2)$, any finite $O(\epsilon)$ bandwidth of modes is possible. It is the aim of the following analysis to look at some of these. Accordingly, we begin with the modified 'neutral' solutions.

$$\left.\begin{aligned} w_0 &= \{W(X,Y,T)\, e^{i\mathbf{k}.\mathbf{x}} + W^*(X,Y,T)\, e^{-i\mathbf{k}.\mathbf{x}}\} \sin\frac{\pi z}{d}, \\ T_0 &= \frac{\beta_0 d^2}{\kappa(\pi^2 + k^2 d^2)} (W e^{i\mathbf{k}.\mathbf{x}} + W^* e^{-i\mathbf{k}.\mathbf{x}}) \sin\frac{\pi z}{d}, \\ u_0 &= \frac{ik_x \pi}{k^2 d} (W e^{i\mathbf{k}.\mathbf{x}} - W^* e^{-i\mathbf{k}.\mathbf{x}}) \cos\frac{\pi z}{d}, \\ v_0 &= \frac{ik_y \pi}{k^2 d} (W e^{i\mathbf{k}.\mathbf{x}} - W^* e^{i\mathbf{k}.\mathbf{x}}) \cos\frac{\pi z}{d} \\ \frac{p_0}{\rho_r} &= \frac{-\pi\kappa}{k^2 d} \left(\frac{\pi^2}{d^2} + k^2\right) (W e^{i\mathbf{k}.\mathbf{x}} + W^* e^{-i\mathbf{k}.\mathbf{x}}) \cos\frac{\pi z}{d}, \\ \mathbf{k}.\mathbf{x} &= k_x x + k_y y, \end{aligned}\right\} \tag{2.7}$$

where the amplitude W is a slowly varying function of position as well as time, in order to accommodate a description of the sidebands. This technique has been successfully used by Benney & Newell (1967) and Newell (1969) in describing interacting wave packets. The appropriate scaling is

$$X = \epsilon x, \quad Y = \epsilon y, \quad T = \epsilon^2 t. \tag{2.8}$$

It turns out that if slow spatial variation occurs over a distance of $O(\epsilon^{-1})$, then only the variation parallel to $\mathbf{k}$ has an effect at lowest order. For variation perpendicular to the $\mathbf{k}$ direction, which we will discuss in more detail at a later stage, the scale $\sqrt{\epsilon}$ is the appropriate one. With the transformation (2.8) the operators reduce to

$$\left.\begin{aligned} &\frac{\partial}{\partial t} \to \frac{\partial}{\partial t} + \epsilon^2 \frac{\partial}{\partial T}, \\ &\nabla_{1\mathbf{x}} \to \nabla_{1\mathbf{x}} + \epsilon \nabla_{1\mathbf{X}}, \quad \nabla_{1\mathbf{x}} = \left(\frac{\partial}{\partial x}, \frac{\partial}{\partial y}\right), \quad \nabla_{1\mathbf{X}} = \left(\frac{\partial}{\partial X}, \frac{\partial}{\partial Y}\right). \end{aligned}\right\} \tag{2.9}$$

We readily reduce the equation system (2.1)–(2.3) to a single equation by twice taking the curl of the momentum equation and taking its dot product with $\hat{\mathbf{z}}$, the unit vector in the vertical. To remove the temperature from the linear part of the operator, we apply the operator $(\partial/\partial t) - \kappa\nabla^2$ to the resulting equation and obtain

$$\begin{aligned} &\left(\frac{\partial}{\partial t} - \nu\nabla^2\right)\left(\frac{\partial}{\partial t} - \kappa\nabla^2\right)\nabla^2 w - \alpha g(\beta_0 + \epsilon^2\beta_2)\nabla_1^2 w \\ &\qquad = -\alpha g \nabla_1^2 (u.\nabla T) + \left(\frac{\partial}{\partial t} - \kappa\nabla^2\right)[\hat{\mathbf{z}}.(\nabla \times \nabla \times (\boldsymbol{\Omega} \times \mathbf{u})]. \end{aligned} \tag{2.10}$$

We expand the dependent variables as a power series in ϵ,

$$f = \epsilon f_0 + \epsilon^2 f_1 + \epsilon^3 f_2 + \ldots, \quad f = (u, v, w, T, p), \tag{2.11}$$

where the f_0 are the modified neutral solutions of the most unstable mode given by (2.7). The equation (2.10) with the transformations (2.8) and (2.9) now reads

$$\begin{aligned}(\mathscr{L}_0+\epsilon\mathscr{L}_1+\epsilon^2\mathscr{L}_2)(w_0+\epsilon w_1+\epsilon^2 w_2)\\ =-\alpha g\epsilon(\nabla_{1\mathbf{x}}^2+2\epsilon\nabla_{1\mathbf{x}}.\nabla_{1\mathbf{X}})\{\mathbf{u}_0.\nabla T_0+\epsilon(\mathbf{u}_1.\nabla T_0+\mathbf{u}_0.\nabla T_1)\}\\ +\epsilon\left\{\frac{\partial}{\partial t}-\kappa\left(\nabla_{1\mathbf{x}}^2+\frac{\partial^2}{\partial z^2}+2\epsilon\nabla_{1\mathbf{x}}.\nabla_{1\mathbf{X}}\right)\right\}[\tilde{\nabla}\times\tilde{\nabla}\times\{(\boldsymbol{\Omega}_0\times\mathbf{u}_0)\\ +\epsilon(\boldsymbol{\Omega}_1\times\mathbf{u}_0)+\epsilon(\boldsymbol{\Omega}_0\times\mathbf{u}_1)\}.\hat{\mathbf{z}}],\end{aligned}\tag{2.12}$$

where the operators

$$\mathscr{L}_0=\left\{\frac{\partial}{\partial t}-\nu\left(\nabla_{1\mathbf{x}}^2+\frac{\partial^2}{\partial z^2}\right)\right\}\left\{\frac{\partial}{\partial t}-\kappa\left(\nabla_{1\mathbf{x}}^2+\frac{\partial^2}{\partial z^2}\right)\right\}\left(\nabla_{1\mathbf{x}}^2+\frac{\partial^2}{\partial z^2}\right)-\alpha g\beta_0\nabla_{1\mathbf{x}}^2,$$

$$\begin{aligned}\mathscr{L}_1=2\Bigg[&\left\{\frac{\partial}{\partial t}-\nu\left(\nabla_{1\mathbf{x}}^2+\frac{\partial^2}{\partial z^2}\right)\right\}\left\{\frac{\partial}{\partial t}-\kappa\left(\nabla_{1\mathbf{x}}^2+\frac{\partial^2}{\partial z^2}\right)\right\}\\ &-\kappa\left\{\frac{\partial}{\partial t}-\nu\left(\nabla_{1\mathbf{x}}^2+\frac{\partial^2}{\partial z^2}\right)\right\}\left(\nabla_{1\mathbf{x}}^2+\frac{\partial^2}{\partial z^2}\right)\\ &-\nu\left\{\frac{\partial}{\partial t}-\kappa\left(\nabla_{1\mathbf{x}}^2+\frac{\partial^2}{\partial z^2}\right)\right\}\left(\nabla_{1\mathbf{x}}^2+\frac{\partial^2}{\partial z^2}\right)-\alpha g\beta_0\Bigg]\nabla_{1\mathbf{x}}.\nabla_{1\mathbf{X}},\end{aligned}$$

$$\begin{aligned}\mathscr{L}_2=&\left[\left\{\frac{\partial}{\partial t}-\nu\left(\nabla_{1\mathbf{x}}^2+\frac{\partial^2}{\partial z^2}\right)\right\}\left\{\frac{\partial}{\partial t}-\kappa\left(\nabla_{1\mathbf{x}}^2+\frac{\partial^2}{\partial z^2}\right)\right\}-\kappa\left\{\frac{\partial}{\partial t}-\nu\left(\nabla_{1\mathbf{x}}^2+\frac{\partial^2}{\partial z^2}\right)\right\}\left(\nabla_{1\mathbf{x}}^2+\frac{\partial^2}{\partial z^2}\right)\right.\\ &\left.-\nu\left\{\frac{\partial}{\partial t}-\kappa\left(\nabla_{1\mathbf{x}}^2+\frac{\partial^2}{\partial z^2}\right)\right\}\left(\nabla_{1\mathbf{x}}^2+\frac{\partial^2}{\partial z^2}\right)-\alpha g\beta_0\right]\nabla_{1\mathbf{X}}^2\\ &+\left[2\frac{\partial}{\partial t}-(\kappa+\nu)\left(\nabla_{1\mathbf{x}}^2+\frac{\partial^2}{\partial z^2}\right)\right]\left(\nabla_{1\mathbf{x}}^2+\frac{\partial^2}{\partial z^2}\right)\frac{\partial}{\partial T_2}\\ &+4\left[\nu\kappa\left(\nabla_1^2+\frac{\partial^2}{\partial z^2}\right)-\kappa\left\{\frac{\partial}{\partial t}-\nu\left(\nabla_1^2+\frac{\partial^2}{\partial z^2}\right)\right\}-\nu\left\{\frac{\partial}{\partial t}-\kappa\left(\nabla_1^2+\frac{\partial^2}{\partial z^2}\right)\right\}\right]\\ &\times(\nabla_{1\mathbf{x}}.\nabla_{1\mathbf{X}})^2-\alpha g\beta_2\nabla_{1\mathbf{x}}^2,\end{aligned}$$

and

$$\tilde{\nabla}=\nabla_{1\mathbf{x}}+\epsilon\nabla_{1\mathbf{X}},\frac{\partial}{\partial z}.\tag{2.13}$$

The linear balance yields the neutral solution set (2.7). The first non-linear response yields a generation of second harmonics. Before we list these, we note in particular that $\mathscr{L}_1 w_0=0$. The reason for this is that we have chosen $|\mathbf{k}|$ to be the wave-number modulus giving the minimum Rayleigh number

$$R_{\mathrm{cr}}(\alpha g\beta_0 d^4/\nu\kappa).$$

We find the second harmonic response which we will denote by $f_1^{(2)}$ to be

$$\begin{aligned}w_1^{(2)}=u_1^{(2)}=v_1^{(2)}=0,\\ T_1^{(2)}=-\frac{\beta_0 d^3}{2\pi\kappa^2(\pi^2+k^2d^2)}WW^*\sin\frac{2\pi z}{d},\\ p_1^{(2)}=\left\{\frac{\alpha g\beta_0 d^4}{4\pi^2\kappa^2(\pi^2+k^2d^2)}+1\right\}WW^*\cos\frac{2\pi z}{d}+\frac{\pi^2}{k^2d^2}(W^2e^{2i\mathbf{k}.\mathbf{x}}+W^{*2}e^{-2i\mathbf{k}.\mathbf{x}}).\end{aligned}\tag{2.14}$$

In addition, there are free modes generated in T_1 and p_1 due to the dependence of W on the slow horizontal co-ordinates (X, Y). However, these do not return to give 'secular' responses in w_2 and so do not affect the analysis to this stage,

Using (2.7) and (2.14) we find the $O(\epsilon^2)$ balance of (2.12) yields

$$\mathscr{L}_0 w_2 = -\mathscr{L}_2 w_0 + \frac{\alpha g \beta_0 d^2 k^2}{2\kappa^2(\pi^2 + k^2 d^2)} WW^* (We^{i\mathbf{k}.\mathbf{x}} + W^* e^{i\mathbf{k}.\mathbf{x}}) \sin\frac{\pi z}{d} + \text{other terms}, \tag{2.15}$$

with the boundary conditions

$$w_2 = \frac{\partial^2 w_2}{\partial z^2} = \frac{\partial^2 w_2}{\partial z^4} = 0. \tag{2.16}$$

The 'other terms' in (2.15) are higher harmonics and do not contain the eigenfunctions corresponding to the operator with the boundary conditions (2.16). However, the first two terms of the right-hand side of (2.15) involve the natural eigenfunction of the operator $\mathscr{L}_0$, and thus the solvability condition demands

$$\hat{\mathscr{L}}_2 W = \frac{\alpha g \beta_0 d^2 k^2}{2\kappa^2(\pi^2 + k^2 d^2)} W^2 W^*, \tag{2.17}$$

where
$$\hat{\mathscr{L}}_2 = -(\nu + \kappa)\left(\frac{\pi^2}{d^2} + k^2\right)^2 \frac{\partial}{\partial T} + 12\nu\kappa\left(\frac{\pi^2}{d^2} + k^2\right)(\mathbf{k}.\nabla_{\mathbf{X}})^2 + \alpha g \beta_2 k^2. \tag{2.18}$$

We non-dimensionalize as follows:

$$W = (\kappa/d)\overline{W}, \quad \mathbf{k} = \frac{1}{d}\hat{\mathbf{k}} = \frac{\pi}{\sqrt{2}}\frac{1}{d}\hat{\mathbf{n}},$$

$$T = (d^2/\kappa)\overline{T}, \quad \mathbf{X} = d\mathbf{X},$$

and defining $\beta_2 = \chi\beta_0$ and $\nu/\kappa = p$ (the Prandtl number), we have

$$\frac{2(p+1)}{p}\frac{\partial \overline{W}}{\partial T} - 8(\hat{\mathbf{n}}.\nabla_{\mathbf{X}})^2 \overline{W} = (3\pi^2\chi - \overline{W}\overline{W}^*)\overline{W}. \tag{2.19}$$

The only term in this equation which differs from previous analysis (see Segel 1966, for example) is the diffusion term on the left-hand side. Without this term, it is clear that we are dealing with the non-linear response of just the neutral mode $|\hat{\mathbf{k}}| = \pi/\sqrt{2}$. Thus, non-linear solutions are possible for $\chi > 0$, i.e. when $R > R_{\text{cr}}$, and the system resembles a Van der Pol oscillator which is driven to the steady solution

$$\overline{W}\overline{W}^* = 3\pi^2\chi.$$

The solution $\overline{W} = 0$ is unstable.

The above equation (2.19) enables us to look at the package of modes contained within an $O(\epsilon)$ square of the neutral mode $\hat{\mathbf{k}}$, $|\hat{\mathbf{k}}| = \pi/\sqrt{2}$. In the following we are only going to concern ourselves with finite amplitude roll disturbances as we know from Schlüter *et al.* (1965) that hexagons are unstable finite amplitude states save when the viscosity is temperature-dependent or the mean temperature is time-dependent (see Krishnamurti 1968). We may readily normalize time, length, and velocity to yield

$$\frac{\partial W}{\partial T} - \frac{\partial^2 W}{\partial X^2} = (1 - WW^*)W. \tag{2.20}$$

Here we have taken $\hat{\mathbf{n}}$ to be $(1, 0)$ and $\hat{\mathbf{k}}$ to be $(\pi/\sqrt{2}, 0)$. Since the neutral curve is the circle $|\hat{\mathbf{k}}| = \pi/\sqrt{2}$, it is clear that if we allow an $O(\epsilon)$ band of modes in the X direction, an $O(\epsilon^{\frac{1}{2}})$ band is possible in the Y direction (see figure 2). Accordingly, we should have used the scales $X = \epsilon x$, $Y = \sqrt{\epsilon} y$, in the derivation of (2.19), whence we would have obtained

$$\frac{\partial W}{\partial T} - \left(\frac{\partial}{\partial X} - \frac{i}{\sqrt{2}\pi}\frac{\partial^2}{\partial Y^2}\right)^2 W = W - W^2 W^* \tag{2.21}$$

as our solvability condition, where

$$W = W(\epsilon x, \sqrt{\epsilon} y, \epsilon^2 t). \tag{2.22}$$

It will be necessary to use this formulation in order to determine the effects of rolls whose axes are slightly oblique to the axis of the neutral mode. Moreover,

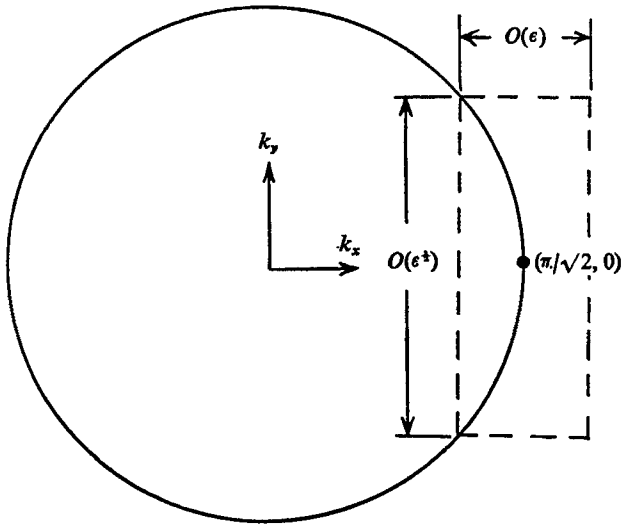

FIGURE 2. The circle $k_x^2 + k_y^2 = \pi^2/2$, showing the possible modes about $k_x = \pi/\sqrt{2}$, $k_y = 0$.

if we have in addition many neutral modes $\hat{\mathbf{k}}_i|_{i=1}^N$, then the equations describing the interaction of the N packages around such modes are

$$\frac{\partial W_i}{\partial T} - \left(\frac{\partial}{\partial X_{(i)}} - \frac{\sqrt{-1}}{\sqrt{2}\pi}\frac{\partial^2}{\partial Y_{(i)}^2}\right)^2 W_i = \left(1 - \sum_{j=1}^{N} W_j W_j - \sum_{\substack{j=1 \\ j\neq i}}^{N} W_j W_j^* \beta_{ij}\right) W_i \quad (i = 1, \ldots N), \tag{2.23}$$

where $|\hat{\mathbf{k}}_i - \hat{\mathbf{k}}_j| = O(1)$, and the coefficients for the case $p = \infty$ are

$$\beta_{ij} = \frac{(5 + \cos\theta_{ij})^2 (1 - \cos\theta_{ij})^2}{(5 + \cos\theta_{ij})^3 - \frac{27}{4}(1 + \cos\theta_{ij})} + \frac{(5 - \cos\theta_{ij})^2 (1 + \cos\theta_{ij})^2}{(5 - \cos\theta_{ij})^3 - \frac{27}{4}(1 - \cos\theta_{ij})},$$

$\cos\theta_{ij} = \hat{\mathbf{n}}_i . \hat{\mathbf{n}}_j$, $\hat{\mathbf{n}}_i$ being the unit vector in the direction $\hat{\mathbf{k}}_i$.

In (2.23) $\partial/\partial X_{(i)}$ refers to the derivative along the unit vector $\hat{\mathbf{n}}_i$ and $\partial/\partial Y_{(i)}$ refers to the derivative normal to $\hat{\mathbf{n}}_i$. The non-linear terms in (2.23) arise only from modal interactions of the type

$$\hat{\mathbf{k}}_i + \hat{\mathbf{k}}_j - \hat{\mathbf{k}}_j = \hat{\mathbf{k}}_i \tag{2.24}$$

as there is no other way in which an interaction

$$\hat{\mathbf{k}}_i + \hat{\mathbf{k}}_j - \hat{\mathbf{k}}_l = \hat{\mathbf{k}}_m \tag{2.25}$$

with $$|\hat{\mathbf{k}}_i^2| = |\hat{\mathbf{k}}_j^2| = |\hat{\mathbf{k}}_l^2| = \tfrac{1}{2}\pi^2,$$

can produce a $\hat{\mathbf{k}}_m$ which is on the curve $\hat{\mathbf{k}}^2 = \frac{1}{2}\pi^2$ for $|\hat{\mathbf{k}}_i - \hat{\mathbf{k}}_j| = O(1)$. However, if we ask only that (2.25) be satisfied to $O(\delta)$ and we allow the $\hat{\mathbf{k}}_i$'s to approach each other arbitrarily closely, then there are many solutions:

$$\hat{\mathbf{k}}_j = \hat{\mathbf{k}}_i + \delta\hat{\boldsymbol{\kappa}}_j, \quad \hat{\mathbf{k}}_l = \hat{\mathbf{k}}_i + \delta\hat{\boldsymbol{\kappa}}_l.$$

This implies $\hat{\mathbf{k}}_m = \hat{\mathbf{k}}_i + \delta(\hat{\boldsymbol{\kappa}}_j - \hat{\boldsymbol{\kappa}}_l)$ from (2.25), whence

$$k_m^2 = \tfrac{1}{2}\pi^2 + O(\delta).$$

We thus obtain in the equation for determining w_2

$$\mathscr{L}_0 w_2 = \exp\left[\mathrm{i}\{\hat{\mathbf{k}} + O(\delta)\}.x\right] \sin \pi z, \quad \hat{\mathbf{k}}^2 = \tfrac{1}{2}\pi^2,$$

where the non-linear forcing is within $O(\delta)$ of being a natural eigenfunction of the operator $\mathscr{L}_0$. Upon integration we would obtain

$$w_2 = O(1/\delta^2),$$

which in the limit $\delta \to 0$ renders the asymptotic expansion (2.11) non-valid. This point has been raised by many authors (Benjamin & Feir 1967; Whitham 1967; Benney & Newell 1967; Newell 1969; Phillips 1967) recently in connexion with resonant wave interactions where it has been noted that a slight (of the order of the non-linearity) detuning of the resonance conditions still leads to the full resonance effect. The packet or finite bandwidth approach essentially enforces a measure on the $\hat{\mathbf{k}}$ space which removes the possibility of ill-conditioned solutions.

3. Modal stability analysis

It is readily seen that solutions of the type

$$W_1 = f_1(T)\, e^{iK_1 X}, \quad W_j = 0, \quad j = 2 \ldots n, \tag{3.1}$$

are possible in (2.23) where we have chosen W_1 to be the amplitude of the mode $\hat{\mathbf{k}}_1 = (\pi/\sqrt{2}, 0)$. The solution of type (3.1) is driven in time to the finite amplitude steady state

$$W_1 = (1 - K_1^2)^{\frac{1}{2}} \quad e^{iK_1 X}, \quad K_1^2 \leqslant 1. \tag{3.2}$$

Note that this solution makes the vertical velocity spatially periodic in the X direction with period $2\pi/(|\hat{\mathbf{k}}_1| + \epsilon K_1)$. Here $K_1 = 0$ corresponds to a mode on the lower branch $\hat{\mathbf{k}}^2 = \frac{1}{2}\pi^2$ of the neutral stability surface corresponding to the critical Rayleigh number and $K_1^2 = 1$ corresponds to the points A_+ and A_- on the

stability curve in figure 1 where the Rayleigh number meets the neutral stability curve. Of relevance is the stability of such solutions. This question has been successfully attacked by Schlüter *et al.* (1965) by strictly modal methods. However, we shall rederive these results in order to: (*a*) show that our approach is consistent with theirs for analyzing the stability of such modal solutions to infinitesimal perturbations; (*b*) put the instabilities discussed by Schlüter *et al.* in perspective with the two-dimensional sideband instabilities demonstrated by Eckhaus; and finally, (*c*) show that the finite band of stable modes disappears as we initiate modal disturbances not on the steady finite amplitude states of these modes but on modes that are in the process of growing to a steady state.

There are three types of instability. The first is a three-dimensional instability whereby the modal solution (3.2) becomes unstable to another discrete roll whose axis makes an $O(1)$ angle with the axis of the mode (3.2). This is readily obtained by substitution of

$$W_1 = (1-K_1^2)^{\frac{1}{2}} e^{iK_1 X} + u_1(T), \tag{3.3}$$
$$W_j = u_j(T),$$

into (2.13), whence we obtain upon linearization

$$\frac{du_j}{dT} = \{1-(1-K_1^2)(1+\beta_{1j})\}u_j, \tag{3.4}$$

which yields

$$u_j \propto \exp\{K_1^2 - \beta_{1j}(1-K_1^2)\}T. \tag{3.5}$$

Exponential growth is possible for the range of wave-numbers

$$K_1^2 > \frac{\beta_{1j}}{1+\beta_{1j}} \tag{3.6}$$

and the maximum growth occurs in the mode $\hat{\mathbf{k}}_j$ when β_{1j} is minimum, for which $\theta_{1j} = \frac{1}{2}\pi$, $\beta_{1j} = 200/473$, and hence $K_1^2 > 200/673$. Thus the most unstable mode is one whose axis is perpendicular to the axis of the roll (3.2). To distinguish this from subsequent instabilities, it will be called a type III instability.

In order to discuss the instability to oblique modes and to two-dimensional sideband modes, it is sufficient to use the equation for the local package in the neighbourhood of $\hat{\mathbf{k}} = (\pi/\sqrt{2}, 0)$. Substituting

$$W = (1-K^2)^{\frac{1}{2}} e^{iKX} + u(X, Y, T), \tag{3.7}$$

into

$$\frac{\partial W}{\partial T} - \left(\frac{\partial}{\partial X} - \frac{i}{\sqrt{2}\pi}\frac{\partial^2}{\partial Y^2}\right)^2 W = (1-WW^*)W, \tag{3.8}$$

we obtain upon linearization

$$\frac{\partial u}{\partial T} - \left(\frac{\partial}{\partial X} - \frac{i}{\sqrt{2}\pi}\frac{\partial^2}{\partial Y^2}\right)^2 u = (1-2p^2)u - p^2 u e^{2iKX}, \tag{3.9}$$

where $p^2 = 1-K^2$ is intrinsically positive by the range of possible solutions (3.2). A set of solutions exists in the form

$$u = v_1(T)\exp[i\{(K+M_X)X + M_Y Y\}] + v_2(T)\exp[i\{(K-M_X)X - M_Y Y\}]$$

as the response of $u^* e^{2iKX}$ to the mode $\exp\{i(K+M_X)X + iM_Y Y\}$ is

$$\exp\{i(K-M_X)X - iM_Y Y\},$$

and the response of $u^*\exp(2iKX)$ to the mode $\exp\{i(K-M_X)X - iM_Y Y\}$ is $\exp\{i(K+M_X)X + iM_Y Y\}$, thus automatically closing the system. (It is helpful also to note that had we perturbed solution (3.2) with functions $u(X, Y, T)$

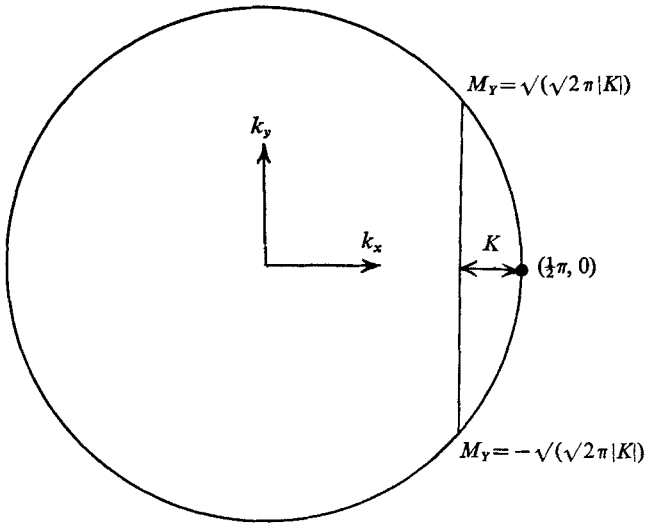

FIGURE 3. The circle $k_x^2 + k_y^2 = \pi^2/2$, showing points of maximum oblique roll growth.

which permitted Fourier transforms, the system again closes as the Fourier transform of $u^*(\mathbf{X})\exp(2i\mathbf{K}.\mathbf{X})$ is $\hat{u}^*(2\mathbf{K}-\mathbf{L})$, where $\hat{u}(\mathbf{L})$ is the Fourier transform of $u(\mathbf{X})$.) Substitution of (3.9) into (3.8) and setting $v_1, v_2 \propto e^{\lambda T}$ gives

$$\lambda = -p^2 - \tfrac{1}{2}U + \sqrt{(p^4 + \tfrac{1}{4}V^2)}, \tag{3.10}$$

where
$$U = \left(K + M_X + \frac{M_Y^2}{\sqrt{2\pi}}\right)^2 + \left(K - M_X + \frac{M_Y^2}{\sqrt{2\pi}}\right)^2 - 2K^2,$$

and
$$V = \left(K + M_X + \frac{M_Y^2}{\sqrt{2\pi}}\right)^2 - \left(K - M_X + \frac{M_Y^2}{\sqrt{2\pi}}\right)^2,$$

$$= 4M_X\left(K + \frac{M_Y^2}{\sqrt{2\pi}}\right).$$

$\lambda(M_X, M_Y : K)$ has relative maxima when

(I) $M_X = 0, \quad M_Y^2 = -\sqrt{2\pi}K; \quad \lambda = K^2;$

(II) $M_X^2 = \dfrac{(3K^2-1)(K^2+1)}{4K^2}, \quad M_Y^2 = 0; \quad \lambda = \dfrac{(3K^2-1)^2}{4K^2}.$

Type I instability is only possible when $K < 0$ (for rolls with length scale larger than the critical roll), and the fastest growing modes are rolls whose axes are oblique to the solution roll but which lie on the circle $\hat{\mathbf{k}}^2 = \frac{1}{2}\pi$ of the neutral stability surface (see figure 3). Type II instability for $K^2 > \frac{1}{3}$ corresponds to the

sideband instability discussed by Eckhaus and is analogous to the sideband instability of the Stokes gravity wave. However, the fastest growing modes do not lie in the close neighbourhood of the original mode but in fact lie within the stability curve $K^2 < \frac{1}{3}$. We summarize with a diagram:

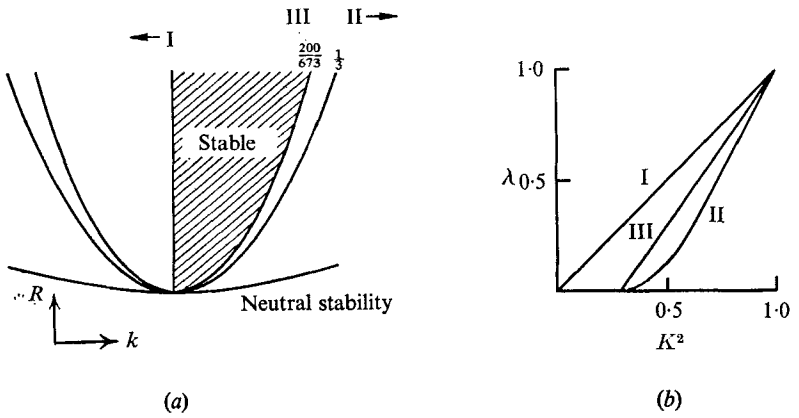

FIGURE 4. Stability diagrams: (*a*) regions of the three types of instability; (*b*) growth rates λ for the various instabilities.

However, it is our feeling that this situation is rather idealistic for the following reason; namely, that while the mode K is growing to its finite amplitude state, it is usually subjected to the same type of perturbations. We wish, therefore, to examine the stability of the time-dependent solution of (3.8) which is of the form

$$W = W_1(T)\, e^{iKX}, \tag{3.11}$$

and whose solution is

$$W_1 W_1^* = \frac{p^2 (W_1 W_1^*)_{T=0}\, e^{2p^2 T}}{p^2 - (W_1 W_1^*)_{T=0} + (W_1 W_1^*)_{T=0} e^{2p^2 T}}, \quad \arg W_1 = \text{constant}, \tag{3.12}$$

where $p^2 = 1 - K^2$.

We note that $W_1 W_1^*$ is a continuous function of time (in fact, analytic) increasing monotonically from its initial value (which may be as close to zero as we wish) to its final amplitude of p^2. Continuity implies that all intermediate values are assumed by the function, and we pose the following question. If at some time T_α at which the amplitude of $W_1 W_1^*$ is $\alpha^2 p^2 (0 < \alpha^2 \leqslant 1)$ we introduce infinitesimal sideband perturbations, then for small times after T_α, how do the growth rates of the perturbations compare with the local growth rate of $W_1(T)$? Accordingly, we set

$$W = W_1(T) \exp(iKX) + \mu W_2(T) \exp\{i(K + M_X) X + iM_Y Y\} + \mu W_3(T) \times \exp\{i(K - M_X) X - iM_Y Y\}, \quad (|\mu| \ll 1), \tag{3.13}$$

into

$$\frac{\partial W}{\partial T} - \left(\frac{\partial}{\partial X} - \frac{i}{\sqrt{2\pi}} \frac{\partial^2}{\partial Y^2}\right)^2 W = W - W^2 W^*. \tag{3.14}$$

Neglecting $O(\mu^2)$ terms, we obtain

$$\frac{dW_1}{dt} = (p^2 - W_1 W_1^*) W_1, \tag{3.15}$$

$$\frac{d}{dT}\begin{bmatrix} W_2 \\ W_3^* \end{bmatrix} = \begin{bmatrix} 1-\left(K+M_X+\dfrac{M_Y^2}{\sqrt{2\pi}}\right)^2 - 2W_1W_1^*, & -W_1^2 \\ -W_1^{*2}, & 1-\left(K-M_X+\dfrac{M_Y^2}{\sqrt{2\pi}}\right)^2 - 2W_1W_1^* \end{bmatrix}\begin{bmatrix} W_2 \\ W_3^* \end{bmatrix}. \tag{3.16}$$

We see from (3.15) that by self-interaction the mode K receives an initial exponential growth $\exp\{\lambda_{S.I}(T-T_\alpha)\}$ from an initial state $W_1 W_1^* = \alpha^2 p^2$, where

$$\lambda_{S.I} = p^2(1-\alpha^2). \tag{3.17}$$

We can find the initial growth of the sideband and oblique perturbation modes from the initial state $W_1 W_1^* = \alpha^2 p^2$, $W_2, W_3 = O(\mu)$, $|\mu| \ll 1$, by giving the matrix in (3.16) its value at time T_α. Since the eigenvalues of the matrix are distinct for all T_α, this step is justifiable from standard theorems in differential equations (see Coddington 1961, p. 224; see also appendix of this paper) by noting that the solution of (3.16) is a continuous function of the parameter W_1 which in turn by (3.15) is clearly a continuous function of time. Thus, in the neighbourhood of T_α, the growth rates of the oblique and sideband modes are given by

$$\exp\{\lambda_{\text{oblique}}(T-T_\alpha)\} \quad \text{and} \quad \exp\{\lambda_{S.B}(T-T_\alpha)\}, \text{ where}$$

$$\text{(I)}\ \lambda_{\text{oblique}} - \lambda_{S.I} = K^2 \quad \text{for} \quad M_X = 0, \quad M_Y^2 = -\sqrt{2\pi}K \quad (K<0), \tag{3.18}$$

$$\text{(II)}\ \lambda_{S.B} - \lambda_{S.I} = \frac{((\alpha^2+2)K^2-\alpha^2)^2}{4K^2} \quad \text{for} \quad M_Y = 0,$$

$$M_X^2 = \frac{((\alpha^2+2)K^2-\alpha^2)((2-\alpha^2)K^2+\alpha^2)}{4K^2}, \tag{3.19}$$

$$K^2 > \frac{\alpha^2}{\alpha^2+2}.$$

A similar calculation for the three-dimensional disturbance perturbing the solution (3.12) at time T_α gives

$$\text{(III)}\ \lambda_{3D} - \lambda_{S.I} = K^2 - \alpha^2\beta_{12}(1-K^2) \quad \text{for} \quad K^2 > \frac{\alpha^2}{\alpha^2+(1/\beta_{12})}. \tag{3.20}$$

We note that in particular for $\alpha^2 = 1$ the results reduce to those found previously in this section. The result of the oblique perturbation remains the same. The range for which the mode K grows faster than the three-dimensional and sideband perturbations decreases to zero with decreasing α^2. Outside this range note that the perturbations are growing exponentially faster than the mode K, which is a further justification for the mathematical treatment described in the previous paragraph. Note in addition that as α^2 gets close to zero all the perturbation modes grow at the same rate.

$$\lambda_{\text{I, II, III}} - \lambda_{S.I} = K^2 = 1-(1-K^2),$$

as in the limit $\alpha^2 \to 0$ they all lie on the curve $\hat{\mathbf{k}}^2 = \pi^2/2$ and grow with their natural growth rate from an infinitesimal perturbation.

We emphasize that the latter analysis of this section has been a local theory in the neighbourhood of T_α but it indicates that the single mode steady solution for $K \neq 0$ is unlikely to be attained. This would suggest that the only *single* mode steady finite amplitude solution which can be attained is that of the most critical mode $K = 0$ (or $\hat{\mathbf{k}}^2 = \pi^2/2$). However, it is still possible to force a mode K to its finite amplitude value *before* crossing to some supercritical Rayleigh number, for in this case, if K lies in the band $0 < K < \sqrt{(200/673)}$, all perturbations will be damped.

Before commenting on the relation of these results with experimental observations, let us point out one of the advantages of the finite bandwidth approach. If we take the three discrete modes (whose interaction leads to the sideband and oblique mode instabilities) $\hat{\mathbf{k}}_1, \hat{\mathbf{k}}_2, \hat{\mathbf{k}}_3$ to be

$$(k+\epsilon K, 0), \quad (k+\epsilon(K+M_X), \sqrt{\epsilon} M_Y), \quad (k+\epsilon(K-M_X), -\sqrt{\epsilon} M_Y),$$

respectively, then a discrete mode analysis would have to include the

$$2\hat{\mathbf{k}}_1 - \hat{\mathbf{k}}_2 = \hat{\mathbf{k}}_3$$

interaction in addition to the

$$\hat{\mathbf{k}}_i + \hat{\mathbf{k}}_j - \hat{\mathbf{k}}_j = \hat{\mathbf{k}}_i$$

interactions. However, substitution of

$$W = W_1 \exp(iKX) + W_2 \exp\{i(K+M_X)X + iM_Y Y\} + W_3 \times \exp\{i(K-M_X)X - iM_Y Y\}$$

into (3.8) automatically incorporates the correct interaction giving rise to the instability. An analysis which examines the competition of two modes close together and which only accounts for the

$$\hat{\mathbf{k}}_i + \hat{\mathbf{k}}_j - \hat{\mathbf{k}}_j = \hat{\mathbf{k}}_i \quad (i,j = 1,2)$$

interactions would lead to incorrect results.

The only experimental situation where instabilities of two-dimensional modes have been observed involved an experiment in which the modes were artificially initiated by the experimenter (see Chen & Whitehead 1968). The instability most clearly observed was in the form of two-dimensional rolls at right angles to the original rolls (and very similar to type III instabilities). This occurred when the original rolls had a wavelength less than the critical value.

Type I instability was not seen as clearly, possibly because its finite amplitude behaviour is not as powerful. However, there was a strong tendency for large two-dimensional rolls to zig-zag, and this could well be a manifestation of growing oblique rolls. If such is true, then finite amplitude effects must alter the oblique rolls at relatively small amplitudes. It would appear doubtful that the type II instability would be noticeable in experimental situations because the two instabilities discussed above have more rapid growth rates. However, in the above experiment, where lateral boundary conditions may well have had an effect, a cell size adjustment was observed.

4. Exact solutions

In the previous section we looked at solutions of spatial period $2\pi/(k+\epsilon K)$. In this section we look at steady periodic envelope solutions of the equations,

$$\frac{d^2W}{dX^2}+W-W^2W^*=0. \tag{4.1}$$

Let $W(X)=r(X)\,e^{i\theta(X)}=u(X)+iv(X)$, r,θ,u,v real and obtain

$$r''-r\theta'^2+r-r^3=0, \tag{4.2}$$

$$r^2\theta'=h \quad (h \text{ constant}), \quad '=d/dX, \tag{4.3}$$

which are the equations for the motion of a particle under a central force field with the potential of a soft spring. Using (4.3) and multiplying (4.2) by r' we obtain upon integration,

$$r'^2=-\frac{h^2}{r^2}-r^2+\tfrac{1}{2}r^4+2E. \tag{4.4}$$

Here E and h correspond to the constant energy and normal angular momentum of the orbit and are the constants of integration. In general the above equation (4.4) yields periodic elliptic functions as solutions. For $E>0$ there is a possibility of a 'solitary' envelope (analogous to the solitary gravity waves) which arises when the cubic on the right-hand side of (4.4) has a double root. Equation (4.4) then has the form

$$r'^2=\tfrac{1}{2}r^2(r^2-r_0^2)^2(r^2-r_1^2) \quad (r_0^2>r_1^2),$$

which has for solution

$$r^2=r_0^2-(r_0^2-r_1^2)\operatorname{sech}^2\frac{r_0^2-r_1^2}{\sqrt{2}}X. \tag{4.5}$$

Another particular solution which is of interest is

$$\left.\begin{aligned} r&=\tanh X/\sqrt{2} \quad (\theta=0).\\ u&=\tanh X/\sqrt{2} \quad (v=0).\end{aligned}\right\} \tag{4.6}$$

As $\tanh X/\sqrt{2}=\pm 1$ for $X=O(\pm 1)$, this solution for moderately large $|X|$ corresponds to rolls of wave-number which have opposite amplitudes as $X\to\pm\infty$, corresponding to a 180° phase change. These two regions of constant amplitude joint smoothly at the origin, where the strength of the rolls decreases to zero. We examine the stability of such a solution to two-dimensional disturbances, namely those independent of the direction of the axes of the rolls. From the discussion in the previous section we know that these two-dimensional solutions outside a certain range of wave-numbers are unstable to infinitesimal three-dimensional disturbances. However, a shear flow in the y direction where the Reynolds number of the shear flow is small will cancel such three-dimensional instabilities and keep the rolls aligned. We set

$$\left.\begin{aligned} u&=\tanh\xi+\hat{u}(\xi)\,e^{-\lambda t},\\ v&=\hat{v}(\xi)\,e^{-\lambda t} \quad (\xi=X/\sqrt{2}),\end{aligned}\right\} \tag{4.7}$$

and we obtain upon linearization the uncoupled set of equations

$$\frac{d^2\hat{u}}{d\xi^2} + (2\lambda - 4 + 6\,\mathrm{sech}^2\,\xi)\,\hat{u} = 0, \tag{4.8}$$

$$\frac{d^2\hat{v}}{d\xi^2} + (2\lambda + 2\,\mathrm{sech}^2\,\xi)\,\hat{v} = 0. \tag{4.9}$$

Our problem is to determine eigenvalues λ for which (4.8) and (4.9) are non-trivially satisfied and we restrict $\hat{u}, \hat{v}$, and their first derivatives to be bounded at $\pm\infty$. Let us first discuss (4.8), which tests the stability of the solution to rolls either in phase or π out of phase with the solution. We prove first that the eigenvalues are real. Multiplying (4.8) by $\hat{u}$ and subtracting the complex conjugate equation we have

$$\frac{d}{d\xi}\left(\hat{u}^*\frac{d\hat{u}}{d\xi} - \hat{u}\frac{d\hat{u}^*}{d\xi}\right) + 2(\lambda - \lambda^*)\,\hat{u}\hat{u}^* = 0. \tag{4.10}$$

If $\hat{u}$ is bounded at $|\infty|$ ($\mathrm{Re}\,\lambda > 2$), then applying the limit

$$\lim_{X\to\infty}\frac{1}{X}\int_{-X}^{X}$$

to (4.10) we find $\lambda = \lambda^*$. If $\hat{u}$ goes to zero at $|\infty|$ then integrating (4.10) between $-\infty$ and ∞ again implies $\lambda = \lambda^*$ and hence λ real. It is clear for $\lambda > 2$ that the solutions will be bounded at $|\infty|$. Instability will only arise for values of $\lambda < 0$. However, it may be possible for $\lambda < 2$ that for certain values of λ the decaying exponential solution is valid for both ends of the ξ axis. This question is readily resolved by making the substitution

$$\tanh\xi = t, \tag{4.11}$$

whereupon (4.8) becomes

$$(1-t^2)^2\frac{d^2\hat{u}}{dt^2} - 2t(1-t^2)\frac{d\hat{u}}{dt} + (2\cdot3(1-t^2) - (4-2\lambda))\,\hat{u} = 0, \tag{4.12}$$

which is the associated Legendre equation. Solutions which are bounded at infinity only occur when $4-2\lambda \leqslant 4$ or for $\lambda \geqslant 0$. In fact the eigenvalues are $\lambda = 0, \frac{3}{2}, 2$ with corresponding eigenfunctions $P_2^2(t)$, $P_2^1(t)$ and $P_2^0(t)$. However, a similar transformation (4.11) in (4.9) yields

$$(1-t^2)^2\frac{d^2\hat{v}}{dt^2} - 2t(1-t^2)\frac{d\hat{v}}{dt} + (1\cdot2(1-t^2) + (-2\lambda))\,\hat{v} = 0,$$

which has solutions $P_1^1(t)$ and $P_1^0(t)$ with eigenvalues of $-\frac{1}{2}$ and 0 respectively. We can prove $-\frac{1}{2}$ is indeed a minimum eigenvalue by looking at the variational problem for (4.9) which is

$$2\lambda = \left\{\int\left(\frac{d\hat{v}}{d\xi}\right)^2 d\xi - 2\int \mathrm{sech}^2\,\xi\,\hat{v}^2\,d\xi\right\}\Big/\int\hat{v}^2\,d\xi.$$

Using the method of multiplicative variation by setting

$$v = \mathrm{sech}\,\xi\,V,$$

we can easily show

$$2\lambda + 1 \geqslant \frac{\int \mathrm{sech}^2\,\xi\,V'^2\,d\xi}{\int \mathrm{sech}^2\,\xi\,V^2\,d\xi} \quad \text{for} \quad \mathrm{sech}^2\,\xi\tanh\xi\,V(\xi)\Big|_{-\infty}^{\infty} = 0,$$

and thus we have in particular the result which will be useful later

$$\int_{-\infty}^{\infty}\left(\frac{d\hat{v}}{d\xi}\right)^2 d\xi - 2\int_{-\infty}^{\infty}\operatorname{sech}^2\xi\hat{v}^2 d\xi \geqslant -\int\hat{v}^2 d\xi. \tag{4.13}$$

Thus it would appear that the solution $u = \tanh\xi$ becomes unstable to rolls $\frac{1}{2}\pi$ out of phase which grow like $e^{\frac{1}{2}t}\operatorname{sech}\xi$. We should remember that for this eigenvalue the solution to (4.8) is $\hat{u} = 0$. Thus the instability appears in the region of the ξ plane where the strength of the rolls is weak and manifests itself in the nature of a 'jetlike' profile. However, from the nature of the non-linear terms in (4.1) we might expect that the sech ξ solution would only grow to a finite amplitude analogous somewhat to the discrete mode solution discussed in § 3.

Thus we might expect solutions of the form

$$u = \tanh\xi, \quad v = \operatorname{sech}\xi. \tag{4.14}$$

Such solutions are not possible for the homogenous system (4.2) but are possible by including a steady forcing term in (4.1) whose real and imaginary parts are

$$f(1+f)^{\frac{1}{2}}\tanh\xi, \quad f^{\frac{1}{2}}(f-\tfrac{1}{2})\operatorname{sech}\xi \quad (f>0).$$

Such a forcing term can arise from a heat source within the fluid of the form

$$\epsilon^2[F(X/\sqrt{2})\,e^{ikx}+(*)]\sin\pi z,$$

F = some external forcing function. Indeed in many situations both in the laboratory and in the real world we do have forced convection. The equation (4.2) becomes

$$\left.\begin{aligned} 2\frac{\partial u}{\partial t} - \frac{\partial^2 u}{\partial\xi^2} &= 2(1-u^2-v^2)\,u + 2f(1+f)^{\frac{1}{2}}\tanh\xi,\\ 2\frac{\partial v}{\partial t} - \frac{\partial^2 v}{\partial\xi^2} &= 2(1-u^2-v^2)\,v + 2(f-\tfrac{1}{2})f^{\frac{1}{2}}\operatorname{sech}\xi),\end{aligned}\right\} \tag{4.15}$$

which system has for solution

$$\bar{u} = (1+f)^{\frac{1}{2}}\tanh\xi, \quad \bar{v} = f^{\frac{1}{2}}\operatorname{sech}\xi. \tag{4.16}$$

If we test the stability of such a solution by setting

$$u = \bar{u} + \hat{u}(\xi)\,e^{-\lambda t}, \quad v = \bar{v} + \hat{v}(\xi)\,e^{-\lambda t},$$

we get the coupled pair of equations

$$\frac{d^3\hat{u}}{d\xi^2} + [(2\lambda - 4 - 6f) + (6+4f)\operatorname{sech}^2\xi]\,\hat{u} - 4f^{\frac{1}{2}}(1+f)^{\frac{1}{2}}\operatorname{sech}\xi\tanh\xi\hat{v} = 0, \tag{4.17}$$

$$\frac{d^2\hat{v}}{d\xi^2} + [(2\lambda - 2f) + (2-4f)\operatorname{sech}^2\xi]\,\hat{v} - 4f^{\frac{1}{2}}(1+f)^{\frac{1}{2}}\operatorname{sech}\xi\tanh\xi\,\hat{u} = 0. \tag{4.18}$$

We of course are interested in the possibility of solutions for $\lambda < 0$ (again, it can readily be shown that λ is real) and in particular $\lambda < f$ in which case $\hat{u}$ and $\hat{v}$ are

not only bounded at (∞) but also asymptotic to zero there. Hence we can write the variational statement

$$2\lambda = \frac{1}{\int \hat{u}^2\,d\xi + \int \hat{v}^2\,d\xi}\left\{\int \hat{u}'^2\,d\xi + \int \hat{v}'^2\,d\xi + (4+6f)\int \hat{u}^2\,d\xi + 2f\int \hat{v}^2\,d\xi \right.$$
$$- (6+4f)\int \operatorname{sech}^3\xi\hat{u}^2\,d\xi - (2-4f)\int \operatorname{sech}^2\xi\hat{v}^2\,d\xi$$
$$\left. + 8f^{\frac{1}{2}}(1+f)^{\frac{1}{2}}\int \operatorname{sech}\xi\tanh\xi\,\hat{u}\hat{v}\,d\xi)\right\}$$
$$= \frac{1}{\int \hat{u}^2\,d\xi + \int \hat{v}^2\,d\xi}\left\{\int \hat{u}'^2\,d\xi + 2f\int \hat{u}^2\,d\xi - 2\int \operatorname{sech}^2\xi\hat{u}^2\,d\xi \right.$$
$$+ \int \hat{v}'^2\,d\xi + 2f\int \hat{v}^2\,d\xi - 2\int \operatorname{sech}^2\xi\,\hat{v}^2\,d\xi$$
$$\left. + 4\int [(1+f)^{\frac{1}{2}}\tanh\xi\hat{u} + f^{\frac{1}{2}}\operatorname{sech}\xi\hat{v}]^2\,d\xi\right\}$$

upon completing the square. Using (4.13) we have

$$2\lambda \geqslant 2f-1, \tag{4.19}$$

where the inequality sign is strict save for $f = 0$ as the function $(\operatorname{sech}\xi)$, which makes the equality hold in (4.14), keeps the perfect square above strictly positive. We notice also for $f = 0$, we regain the result for no forcing, namely $\lambda \geqslant -\frac{1}{2}$. Thus for $f \geqslant \frac{1}{2}$ we have absolute stability. For $f = \frac{1}{2}$ we see that only forcing on the u component is present but this leads to a v component. Where the $u = \tanh\xi$ solution is weak namely at $\xi = 0$, the $v = \operatorname{sech}\xi$ solution is stronger and *vice versa*. For large $|\xi|$ the rolls are of scale $2\pi/k$ except that the sense of rotation of corresponding roll couplets is reversed on opposite sides of the $\xi = 0$ axis. Near the centre the predominant rolls are those which are $\frac{1}{2}\pi$ out of phase with the rolls far away from the origin and whose envelope has a jetlike profile.

It is of interest to inquire not only into the existence and stability of solutions but also their realizability, namely what initial conditions lead to these kinds of steady solutions? As long as the field is kept two-dimensional (and here again we invoke the notion of a shear flow to keep the rolls aligned), then equations (4.15) are exact modal equations for the whole flow. Therefore, we can treat initial-boundary value problems purely from the standpoint of physical space. This is clearly an advantage over the modal or transform approach as the latter leads to the difficulty of galloping inflation (i.e. quadratic interaction of n modes yields $\frac{1}{2}n(n+1)$ modes, etc.) due to the non-linear terms. In order to show the solutions (4.16) realizable we choose the initial conditions $(f = \frac{1}{2})$:

$$u = \sqrt{\left(\frac{3}{2}\right)}\frac{2X}{L} + 0{\cdot}5\sin\frac{2\pi X}{L}, \quad X = \sqrt{2}\xi,$$
$$v = 0{\cdot}5\cos\frac{\pi X}{L},$$

and boundary conditions

$$-u(-\tfrac{1}{2}L,t) = u(\tfrac{1}{2}L,t) = \sqrt{(\tfrac{3}{2})},$$
$$v(-\tfrac{1}{2}L,t) = v(\tfrac{1}{2}L,t) = 0,$$

with $L = 200$. A numerical solution reached the steady solutions

$$u = \sqrt{\tfrac{3}{2}}\tanh\xi, \quad v = \sqrt{\tfrac{1}{2}}\operatorname{sech}\xi$$

after a short time.

It is of interest to discuss the reasons for these solutions being attained. It seems that as far as possible the flow tends to choose as its length scale the

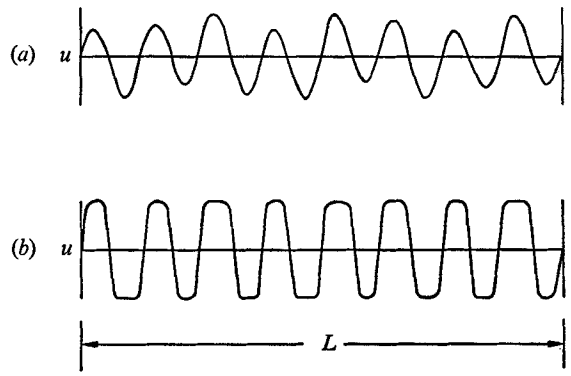

FIGURE 5. Evolution of amplitude function $u(\xi, t)$ from the initial state.
$u = 0{\cdot}2\sin(6\pi/L)\xi + 0{\cdot}8\sin(16\pi/L)\xi$. (*a*) $t = 0$, (*b*) $t = 8{\cdot}0$.
Note that the final length scale is approximately $L/16$.

basic neutral wavelength of the most excited disturbance subject to initial and boundary conditions and the forces applied. For simplicity let us choose the equation

$$\frac{\partial u}{\partial t} - \frac{\partial^2 u}{\partial \xi^2} = (1-u^2)\,u \tag{4.20}$$

with boundary conditions $u(-\frac{1}{2}L,t) = u(\frac{1}{2}L,t) = 0\,(L = 200)$.

We represent the initial conditions by a Fourier series

$$\sum_n a_n \sin\frac{n\pi}{L}(\xi + \tfrac{1}{2}L)\Big\}_{n=1}^{\infty}.$$

For the purpose of example we take the two modes $a_6 = a_{16} = 1$, all others zero, so that the initial curve contains the basic length scales $\frac{1}{6}L, \frac{1}{16}L$. From (4.20) we see there are two forces tending to change $u(\xi,t)$: (*a*) the Van der Pol term $(1-u^2)\,u$ which tends to drive the solution to ± 1; (*b*) the curvature term $\partial^2 u/\partial\xi^2$ which tends to iron out kinks in the initial curve. If we begin as in figure 5 with the initial conditions

$$u = 0{\cdot}2\sin\frac{6\pi}{L}\xi + 0{\cdot}8\sin\frac{16\pi}{L}\xi,$$

the final result has a dominant scale of $\frac{1}{16}L$, but the shape of a square wave with hyperbolic tangent smoothing. This corresponds with a mode

$$K = (16\pi/200) \sim 0{\cdot}25,$$

which lies well within the parabolic stability bound for sideband disturbances $K^2 = \frac{1}{3}$. As the amplitude of the initial mode is large enough, no instability takes place. Similarly, if we begin as in figure 6 with

$$u = 0{\cdot}8 \sin \frac{6\pi}{L}\xi + 0{\cdot}2 \sin \frac{16\pi}{L}\xi,$$

the final form is again rectangular with the dominant scale $\frac{1}{16}L$. However, if we begin as in figure 7 with the amplitudes of the two modes equal,

$$u = 0{\cdot}5 \sin \frac{6\pi}{L}\xi + 0{\cdot}5 \sin \frac{16\pi}{L}\xi,$$

we note that the curvature terms tend to iron out the kinks due to the shorter scale (see arrows in figure), so that the dominant scale in the final solution is that of the larger wavelength. Note, however, that the finite amplitude of the perturbing smaller scale has slightly lengthened the dominant scale

$$(\text{due to } \sin A + \sin B = 2 \sin (A+B)/2 \cos (A-B)/2)$$

so that this scale no longer fits by itself into the box. Thus, in order to fit boundary conditions, the higher harmonics are generated in the neighbourhood of the boundaries.

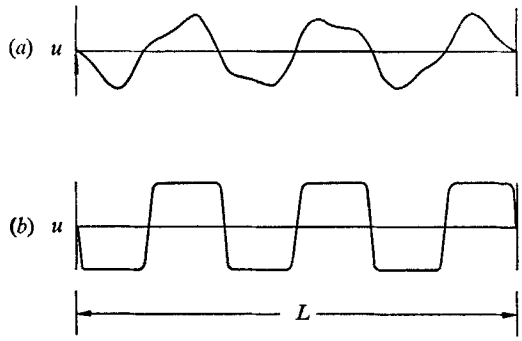

FIGURE 6. Evolution of amplitude function $u(\xi, t)$ from the initial state.
$u = 0{\cdot}8 \text{ in } (6\pi/L)\,\xi + 0{\cdot}2 \sin (16\pi/L)\,\xi$. (*a*) $t = 0$, (*b*) $t = 8{\cdot}0$.
Note that the final length scale is about $L/6$.

These results are perhaps contrary to those which one might expect from an initial examination of the linear eigenvalue problem posed by (2.20) with boundary conditions

$$W(0, T) = W(L_X, T) = 0. \tag{4.21}$$

It is convenient to use the dimensionless but not the normalized form of (2.20) with $\hat{\mathbf{n}} = (1, 0)$ which in the linear approximation is

$$2\frac{p+1}{p}\frac{\partial \overline{W}}{\partial T} - 8\frac{\partial^2 \overline{W}}{\partial X^2} = 3\pi^2 \chi \overline{W}, \tag{4.22}$$

where $\epsilon^2\chi = (R - R_{\text{cr}})/R_{\text{cr}}$ and χ is the eigenvalue. The solution

$$\overline{W} = e^{\sigma t} \sin \frac{n\pi}{L_X} X \tag{4.23}$$

satisfies the boundary condition (4.21) and for $\sigma = 0$ leads to the relation

$$\frac{n^2\pi^2}{L_X^2} = 3\frac{\pi^2\chi}{8}. \tag{4.24}$$

Defining $$K_n^2 = \frac{n^2\pi^2}{L_X^2}$$

we have $$R^{(n)} - R_{\rm cr} = \frac{8}{3\pi^2} R_{\rm cr} K_n^2, \tag{4.25}$$

which implies that the K_n lie on the neutral stability curve (figure 1). This can be easily verified by expanding

$$R = \frac{(k^2+\pi^2)^3}{k^2}$$

in the neighbourhood of $k_{\rm cr}$. Thus the minimum Rayleigh number for convection subject to sidewall boundary conditions is the Rayleigh number corresponding to the wave-numbers $k_{\rm cr} \pm \epsilon K_1$ with $K_1^2 = \pi^2/L_X^2$ closest to $k_{\rm cr}$. If L_X were equal to

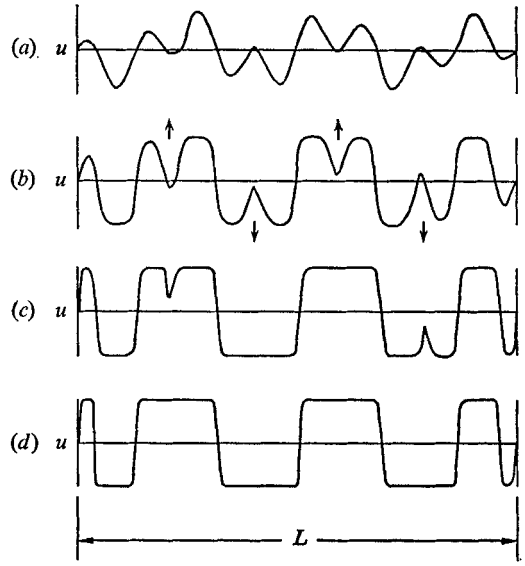

FIGURE 7. Evolution of amplitude function $u(\xi, t)$ from the initial state.

$u = 0{\cdot}5 \sin(6\pi/L)\,\xi + 0{\cdot}5 \sin(16\pi/L)\,\xi$.(*a*) $t = 0$, (*b*) $t = 1{\cdot}6$, (*c*) $t = 5{\cdot}6$, (*d*) $t = 8{\cdot}0$. Note that length scales of both $L/6$ and $L/16$ are noticeable.

$(2\pi/k_{\rm cr})N$, N a large integer, one might infer that convection could automatically fit in the box and the critical Rayleigh number would be the usual $R_{\rm cr}$ for an infinite box. But in order to satisfy both boundary conditions $u = w = 0$ (see (2.7)); this is not so. The convective pattern that arises in a finite box is made up of two scales, $2\pi/(k_{\rm cr} \pm \epsilon K_1)$ with K_1 corresponding to the longest mode that fits in the box. The combination of these two scales yields the eigenfunction structure $e^{ik_{\rm cr}x} \sin K_1 X$. The sinusoidal eigenfunction solution $W = \sin K_1 X$ (unlike the case of a single mode) does not persist when substituted into the cubic non-linear

term W^2W^*. The third harmonic is generated, and this and higher harmonics distort the initial sinusoidal profile, leading to the final shapes we obtained with the numerical experiments.

The linear eigenvalue problem taking account of the slight three-dimensionality can be similarly performed on (2.22) by using the eigenfunction structure:

$$W = \exp(\sigma T)\exp\left\{-i\frac{1}{\sqrt{(2\pi)}}K_Y^{(m)^2}X\right\}\sin K_X^{(n)}X\sin K_Y^{(m)}Y,$$

$$K_X^{(n)} = \frac{n\pi}{L_X}, \quad K_Y^{(m)} = \frac{m\pi}{L_Y}. \tag{4.26}$$

This leads to exactly the same relation as (4.23) as the Y dependence does not play a role in determining the Rayleigh number but only in splitting the package into two which are centred at

$$\left(\frac{\pi}{\sqrt{2}} - \frac{\epsilon}{\sqrt{2\pi}}K_Y^{(m)^2}, \quad \pm\sqrt{\epsilon}K_Y^{(m)}\right).$$

5. Conclusion

Whereas we have used as a model the convection problem, the basic ideas used in this approach are relevant to problems where a continuous band of modes is possible. Examples of such applications occur in dispersive wave theory when there is no *a priori* quantization of modes. Indeed we know that the sideband modes play the dominant role in non-linear wave interaction and are responsible for destabilizing the well-known Stokes gravity wave for sufficiently deep water. In this latter case a discrete mode analysis leads immediately to the excitation of all higher harmonics of the sideband modes and a wave packet approach is required in order to attain any steady solution (Benney & Newell 1967). In the problem of convective instability in a rotating system (or with superposed magnetic field) growing oscillations are the predominant instability for sufficiently low Prandtl number. In this case the solvability equation contains dispersion and frequency modification terms in addition to diffusion and Van der Pol forcing. In addition it is necessary to move with the group velocity of each disturbance. Of interest would be the competing effects of the dispersive wave sideband instability when the fastest growing modes lie in the immediate neighbourhood of the initial mode itself and the sideband instability mechanism described in §3 when the fastest growing mode is chosen discretely from a balance of diffusion and Van der Pol forcing.

Indeed, were the neutral stability régimes derived from the Orr–Sommerfeld equation for the description of the instability of infinitesimal disturbances in parallel flows realizable physically, then these ideas would be equally valid and the solvability equation would parallel that of the overstable convection described in the previous paragraph.

As mentioned in the introduction, the statistical initial value problem is also of interest, as the initial values of the disturbances are usually quite random in nature. This would closely parallel similar work done on Burger's equation

(Lange 1968) for late decay with the difference that the statistical moments of the amplitudes themselves in general grow in time. We believe that the effect of the non-linear coupling will be to drive all the energy toward low sideband wave-numbers (or back to the most excited critical mode).

At the risk of over-emphasis, let us briefly review the results of this work. First, the representation used was that of packages centred around the most unstable modes lying on the minimum curve of the neutral stability diagram $k^2 = \frac{1}{2}\pi^2$. This had the advantage that the only non-linear modal interactions which we needed to consider were of the type.

$$\hat{\mathbf{k}}_i + \hat{\mathbf{k}}_j - \hat{\mathbf{k}}_j = \hat{\mathbf{k}}_i.$$

The resulting solvability conditions showed clearly that spatial non-uniformities were propagated by diffusion. Numerical experiments confirmed this. The results of Schlüter *et al.* (1965) and those of Eckhaus (1965) were rederived, but we have shown the unlikelihood of modes other than $K = 0$ ever reaching the final state if the fluid is initially motionless. However, the main purpose of this work was not to discuss modal solutions but to attain a wider class of solutions which are both realizable and stable. The advantage of the technique was demonstrated clearly for the case of two dimensions, when a single equation was sufficient to describe the evolution of the flow from a wide variety of initial and boundary conditions.

The results of §4 are by no means exhaustive but contain what we believe to be the essential features for smoothing discontinuities which may be forced on the system by external conditions. Other features salient to a slight three-dimensionality can be noted by searching for solutions to (2.21). Solutions to this do exist and take the form of sech Y tanh Y. This corresponds to rolls whose spin varies along the axis of the roll and which spin is in opposite directions on different sides of zero. Although we have not tested the stability of these solutions, it is of interest to note that they do vanish for sufficiently large Y, thus allowing boundary conditions to be satisfied. Perhaps they can be reached if the initial information is confined locally in the neighbourhood of the mode vector

$$\hat{\mathbf{k}} = (\pi/\sqrt{2}, 0)$$

or equivalently may be the final state reached by the oblique mode instabilities discussed in §3.

The authors wish to thank Fritz Busse for the many helpful discussions. This work was supported in part by the National Science Foundation, Atmospheric Sciences Section, under Grant GA-849.

Appendix

We include a brief section in order to justify more rigorously the mathematical treatment in §3. We have from (3.16) the vector differential equation

$$\frac{dy}{dT} = A(W(T))y, \tag{A 1}$$

where A is the matrix given in (3.16). We wish to show that in the local neighbourhood of T_α, $\{W(T_\alpha) = W_\alpha = \alpha p\}$ the solutions to (A 1) are arbitrarily close to the solutions of the system

$$\frac{dz}{dT} = A(W(T_\alpha))\, z, \tag{A 2}$$

where the initial conditions at $T = T_\alpha$ on y and z are the same. We may write (A 1) as

$$\frac{dy}{dT} = A(W(T_\alpha))\, y + (A(W(T)) - A(W(T_\alpha)))\, y, \tag{A 3}$$

such that (A 2) and (A 3) may be written

$$\frac{dy}{dT} = f(T, y(T)), \tag{A 4}$$

$$\frac{dz}{dT} = g(T, z(T)), \tag{A 5}$$

where

$$\|f - g\| < \epsilon \quad \text{for} \quad |T - T_\alpha| < \delta, \tag{A 6}$$

the double brackets representing some norm of the difference of the vector functions f and g. In addition we ask that $f(T, y(T))$ satisfy the Lipschitz conditions in the neighbourhood of T_α

$$\|f(T, y(T)) - f(T, z(T))\| \leqslant K \|y(T) - z(T)\|, \tag{A 7}$$

which is clearly so since f is linear in y. Integrating (A 4) and (A 5) from $T = T_\alpha$, and subtracting we obtain

$$y(T) - z(T) = \int_{T_\alpha}^{T} [f(s, y(s)) - f(s, z(s)) + f(s, z(s)) - g(s, y(s))]\, ds \quad (T > T_\alpha).$$

Taking the norm and using (A 6) and (A 7) we have

$$\|y - z\| \leqslant K \int_{T_\alpha}^{T} \|y - z\|\, ds + \epsilon (T - T_\alpha). \tag{A 8}$$

Define

$$E = \int_{T_\alpha}^{T} \|y - z\|\, ds.$$

We obtain

$$\frac{dE}{dT} - KE \leqslant \epsilon (T - T_\alpha),$$

which implies upon integration, since $E(T_\alpha) = 0$, that

$$E \leqslant -\frac{\epsilon}{K}(T - T_\alpha) + \frac{\epsilon}{K}(e^{K(T - T_\alpha)} - 1). \tag{A 9}$$

Resubstituting in (A 8) we have

$$\|y - z\| \leqslant \frac{\epsilon}{K}(e^{K(T - T_\alpha)} - 1).$$

Then the solutions to (A 2) and (A 3) are arbitrarily close provided ϵ is sufficiently small. But

$$\epsilon = \max_{T_\alpha < T < T_\beta} \|A(W(T)) - A(W(T_\alpha))\|$$

$$= \max_{T_\alpha < T < T_\beta} \left\| \frac{dA}{dW} \right\| \left\| \frac{dW}{dT} \right\| |T - T_\alpha|.$$

This means that the faster the basic solution W grows in the neighbourhood of T_α the smaller we must take the neighbourhood (T_α, T_β). However, since the perturbation solutions are growing exponentially faster than the basic flow in the ranges of interest specified in (3.18), (3.19) and (3.20) we do not need a large time interval before the perturbations have significantly changed the flow field.

REFERENCES

Benjamin, T. B. & Feir, J. E. 1967 *J. Fluid Mech.* **27**, 417.

Benney, D. J. & Newell, A. C. 1967 *J. Math. Phys.* **46**, 133.

Chen, M. M. & Whitehead, J. A. 1968 *J. Fluid Mech.* **31**, 1.

Coddington, E. A. 1961 *An Introduction to Ordinary Differential Equations*. New Jersey: Prentice-Hall.

Eckhaus, W. 1965 *Studies in Non-linear Stability Theory*. New York: Springer-Verlag.

Koschmieder, E. L. 1966 *Beitr. Phys. Atmos.* **39**, 1.

Krishnamurti, R. E. 1968 *J. Fluid Mech.* **33**, 445.

Lange, C. 1968 Ph.D. Thesis, Part II. Massachusetts Institute of Technology.

Newell, A. C. 1968 *J. Fluid Mech.* **35**, 255.

Phillips, O. M. 1967 *Proc. Roy. Soc.* A **299**, 104.

Schlüter, A., Lortz, D. & Busse, F. 1965 *J. Fluid Mech.* **23**, 129.

Segel, L. A. 1966 In *Non-Equilibrium Thermodynamics, Variational Techniques and Stability*, ed. by R. J. Donnelly, R. Herman and I. Prigogine. University of Chicago Press.

Silveston, P. L. 1958 *Forsch. Ing. Wes.* **24**, 29–32, 59–69.

Whitham, G. B. 1965 *Proc. Roy. Soc.* A **283**, 238.

Whitham, G. B. 1967 *Proc. Roy. Soc.* A **299**, 6.